Journal of Materials Science and Chemical Engineering, 2025, 13(10), 38-61
https://www.scirp.org/journal/msce
ISSN Online: 2327-6053
ISSN Print: 2327-6045

Assessment of (2E)-1-(4-Methoxyphenyl)-3-(2-Phenyl H-Imidazo [1, 2-a] Pyridine-3-yl) Prop-2-en-1-One Adsorption for Aluminum Corrosion Inhibition in Hydrochloric Acid: Gravimetric, Thermodynamic, and DFT Study

Mbouillé Cissé[1*], Souleymane Bamba[1], Amadou Kouyaté[1], Mougo André Tigori[1], Kouadio Achille Yao[1], Bini Kouamé Dongui[1], Paulin Marius Niamien[2]

[1]Laboratoire des Sciences et Technologies de l'Environnement, UFR Environnement, Université Jean Lorougnon Guédé, Daloa, Côte d'Ivoire
[2]Laboratoire de Constitution et de Réaction de la Matière, UFR SSMT, Université Félix Houphouët-Boigny, Abidjan, Côte d'Ivoire
Email: *mbouille.cisse07@gmail.com

How to cite this paper: Cissé, Mb., Bamba, S., Kouyaté, A., Tigori, M.A., Yao, K.A., Dongui, B.K. and Niamien, P.M. (2025) Assessment of (2E)-1-(4-Methoxyphenyl)-3-(2-Phenyl H-Imidazo [1, 2-a] Pyridine-3-yl) Prop-2-en-1-One Adsorption for Aluminum Corrosion Inhibition in Hydrochloric Acid: Gravimetric, Thermodynamic, and DFT Study. *Journal of Materials Science and Chemical Engineering*, **13**, 38-61.
https://doi.org/10.4236/msce.2025.1310003

Received: August 26, 2025
Accepted: October 28, 2025
Published: October 31, 2025

Abstract

The present study evaluates the adsorption properties of (2E)-1-(4-Methoxyphenyl)-3-(2-Phenyl H-Imidazo[1, 2-*a*] Pyridine-3-yl)prop-2-en-1-one (MPIP) on aluminum corrosion in acid medium (HCl 1 M) at different temperatures. This study was assessed by gravimetric tests and density functional theory (DFT). Gravimetric measurements reveal that the compound's effectiveness increases with concentration but decreases with increasing temperature, suggesting a predominant physical adsorption mechanism. Thermodynamic analysis confirms the spontaneous and exothermic nature of the process, highlighting Langmuir-type adsorption. Theoretical study based on DFT identified the compound's descriptor parameters (E_{HOMO}, E_{LUMO}, energy gap, global hardness and softness), corroborating its chemical reactivity and propensity to interact with the metal surface. Finally, experimental and computational results indicate that the compound studied is a promising, environmentally-friendly corrosion inhibitor for the protection of aluminum in acidic environments.

Keywords

(2E)-1-(4-Methoxyphenyl)-3-(2-Phenyl H-Imidazo [1, 2-a] Pyridine-3-yl) Prop-2-en-1-One (MPIP), Aluminum Corrosion, Gravimetric Measurements, Density Functional Theory (DFT), Environmentally-Friendly

1. Introduction

Metals in service often give a superficial impression of permanence, but all except gold are chemically unstable in almost natural environments. Wear and corrosion are common forms of damage in engineering, causing material deterioration and, consequently, a degradation of its functional properties, whether mechanical, electrical, optical, esthetic, or other [1] [2]. Thus, the successful use of materials in technical and commercial applications depends on protective mechanisms.

In recent years, during discussions on materials, manufacturers have sought to reduce corrosion of metal equipment by incorporating organic compounds into acidic solutions. This approach aims to control or mitigate the dissolution of such equipment. Thanks to research efforts, several organic corrosion inhibitors have been identified.

Inhibitors, which reduce corrosion on metalic materials, can be divided into three kinds: surfactant inhibitors [3]-[5], organic inhibitors [6]-[13] and inorganic inhibitors [14]-[17]. Heterocyclic inhibitors have many advantages, such as high inhibition efficiency [18]-[20], low price, and easy production.

The choice of effective inhibitors is based on their mechanism of action and their electron-donating capability. Moreover, inhibitory ability is reinforced by the presence of the molecular structure of adsorption active sites with the lone pair and or π orbitals, such as heterocyclic rings containing sulphur, oxygen, phosphorus and/or nitrogen atoms [21]-[25]. These compounds can form either a strong coordination bond with metal atom or a passive film on the surface [26]. Imidazoles and their derivatives represent a significant class of organic compounds, distinguished by the presence of heteroatoms (N and O) and aromatic rings. These molecules are generally considered non-toxic and biodegradable [27]. Previous studies [28] [29] have demonstrated their remarkable anticorrosive properties, which are closely associated with their chemical structure and their ability to inhibit the electrochemical reactions responsible for metal degradation.

The corrosion inhibition of a metal may involve either physisorption or chemisorption of the inhibitor on the metal surface. Electrostatic attraction between the charged hydrophilic groups and the charged active centers on the metal surface leads to physicosorption. Several authors showed that most inhibitors were adsorbed on the metal surface by displacing water molecules from the surface and forming a compact barrier film [30]-[33]. Moreover, several researchers [34] [35] have reported that the inhibitory efficiency of these compounds can be correlated with specific quantum chemical parameters, thereby providing deeper insights into the inhibition mechanism.

The purpose of this paper is aimed to deepen our understanding of corrosion inhibition mechanisms (2E)-1-(4-Methoxyphenyl)-3-(2-Phenyl H-Imidazo [1, 2-*a*] Pyridine-3-yl) prop-2-en-1-one (MPIP), particularly through the phenomenon of adsorption and quantum theory, but also to promote the development of new environmentally friendly corrosion inhibitors that can extend the service life of

aluminum components exposed to corrosive environments [36].

2. Experimental Details

2.1. Materials Preparation

The hydrochloric acid (HCl) 1 M solution was prepared by dilution of HCl 37% of analytical quality with bidistilled water. The material used in this study is 1 cm long aluminum rod. Firstly, the aluminum rod was mechanically abraded with abrasive papers in various grain sizes (from grade 150 to 800); rinsed with bidistilled water, degreased in acetone, washed once again with bidistilled water and dried before their immersion in experimental solution. Concentration range of inhibitor used in the tests was from around 10^{-6} to 10^{-3} mol/L.

The aggressive solution (1.0 M HCl) was prepared by dilution of analytical grade 37% HCl with double-distilled water. Corrosion inhibitor solution is prepared by dissolving the desired heterocyclic weight of inhibitor in 1 M HCl. Four different concentrations, namely, 10^{-3}, 10^{-4}, 10^{-5} and 10^{-6} mol/L by weight are used for the evaluation of corrosion inhibition. Structural formulae of the examined inhibitors are shown in Figure 1.

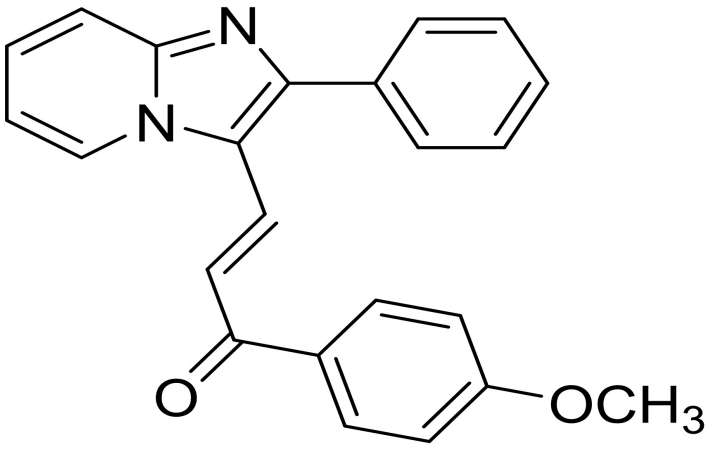

Figure 1. (2E)-1-(4-Methoxyphenyl)-3-(2-Phenyl H-Imidazo [1, 2-a] Pyridine-3-yl) prop-2-en-1-one (MPIP).

2.2. Weight-Loss Measurements

The weight-loss of aluminum rod specimens, 1 cm in 1.0 M HCl, with and without the addition of inhibitors, was determined after 1 h period of immersion at a temperature of 25˚C in air atmosphere without bubbling. Triplicate experiments were performed in each case and the mean value of the weight-loss has been reported.

2.3. Computational Calculations

For convenience reasons, the calculations of isolated molecules were performed with the local Gaussian-type-orbital basis set and Gaussian 09 program especially because the evaluation of vertical ionization potentials and electron affinities involve

calculations of charged species. All calculations were done with DFT at B3LYP level of theory which yields good descriptions of organic molecules. The electronic properties of these structures were studied based on the nature bond orbital analysis (NBO). The calculations of the local and global reactivity indicators of the such as the inhibitor molecules localization of frontier molecular orbitals, E_{HOMO} (Energy of the highest occupied molecular orbital), E_{LUMO} (Energy of the lowest occupied molecular orbital), ΔE_{gap} (Energy gap), I (ionization energy), A (electron affinity), χ (Absolute electronegativity), η (Global hardness), S (Global softness), ω (Global electrophilicity index), ΔN (Fraction of electrons transferred from single inhibitor molecule to metallic surface) and total energy (E_T) were used to explain the electron transfer mechanism between the neutral and protonated forms of inhibitor molecules (NCF & NCCM) and the aluminum surface in acid medium [37] [38].

$$I = -E_{\mathrm{HOMO}} \tag{1}$$

$$A = -E_{\mathrm{LUMO}} \tag{2}$$

$$\Delta E_{L-H} = E_{\mathrm{LUMO}} - E_{\mathrm{HOMO}} \tag{3}$$

$$\chi = \frac{I + A}{2} = \frac{1}{2}\left(E_{\mathrm{HOMO}} + E_{\mathrm{LUMO}}\right) \tag{4}$$

$$\eta = \frac{I - A}{2} = -\frac{1}{2}\left(E_{\mathrm{HOMO}} - E_{\mathrm{LUMO}}\right) \tag{5}$$

$$S = \frac{1}{\chi} = -2/\left(E_{\mathrm{HOMO}} - E_{\mathrm{LUMO}}\right) \tag{6}$$

$$\omega\left(\frac{\mu^2}{2}\right)S = \frac{I + A}{8} \tag{7}$$

$$\Delta N = \frac{\chi_{Al} - \chi_{inh}}{2\left(\eta_{Al} + \eta_{inh}\right)} \tag{8}$$

where χ^{Al} and χ^{inh} represent the absolute electronegativity of Al and the inhibitor molecule respectively, η_{Al} and η_{inh} represent the absolute hardness of Al and the inhibitor molecule, respectively. By assuming that for a metallic $I = A$; because they are softer than the neutral metallic atoms [39]; theorical values for the electronegativity $\chi^{Al} = 4.28$ eV and $\eta_{Al} = 0$ the global hardness were hence used.

3. Results and Discussion

3.1. Weight-Loss Evaluation

Weight-loss tests or Gravimetric tests were carried out to analyze the influence of concentration and temperature on corrosion rate and inhibition efficiency. Weight-losses are expressed in mg per hour per cm^2 of the mild surface area, which were determined in the absence and in the presence of the additives at 25˚C after 1 h of hold time immersion. The highest concentration is sometimes limited by the solubility of the compound. Higher concentrations were not tested even at two consecutive concentrations no further increase is observed in terms of inhibiting efficiency.

The corrosion rates (W), the degree of surface coverage (θ) and the inhibition efficiency IE (%) were calculated using the following expressions:

$$W = \frac{m_0 - m_1}{St} \tag{9}$$

$$\theta = \frac{W_0 - W}{W_0} \tag{10}$$

$$\mathrm{IE}(\%) = \frac{W_0 - W}{W_0} \times 100 \tag{11}$$

- m_0 is the initial mass of the sample before testing.
- m_1 is the final mass of the sample after corrosion.
- S is the total surface area of the sample.
- t is the total corrosion time.
- W_0 is the corrosion rate in the blank solution.
- W is the corrosion rate in the solution containing MPIP.

Figure 2 analysis reveals that the corrosion rate (W) increases with temperature, while it decreases with higher concentrations of the inhibitor. These results highlight the strong dependence of corrosion kinetics on both the temperature of the corrosive medium and the MPIP concentration. Moreover, the data indicate that the thickness of the protective layer formed on the metal surface increases proportionally with the amount of MPIP present.

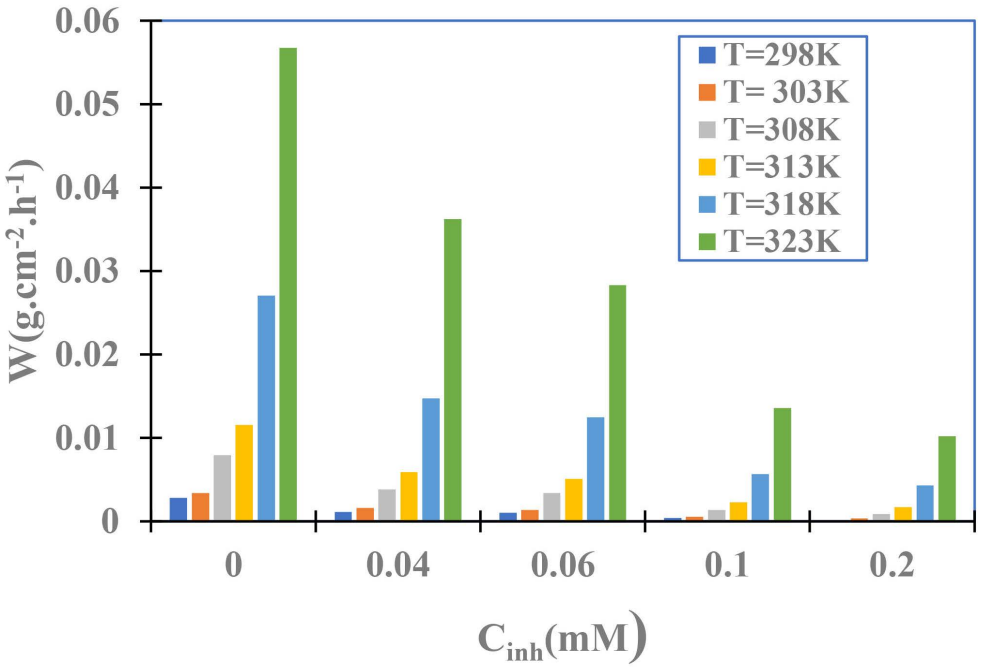

Figure 2. Corrosion rate W with temperature in absence and presence of inhibition.

The protective film formed by the complexation of MPIP with the metal progressively deposits onto the aluminum surface, thereby mitigating its dissolution.

However, the thickness of this film decreases with increasing temperature. These findings underscore the critical influence of temperature and concentration on the corrosion kinetics of aluminum, as well as on the adsorption behavior and inhibitory performance of MPIP at the metal interface, as reported by several studies [40].

Figure 3 illustrates the combined influence of temperature (T) and inhibitor concentration (C_{inh}) on the inhibition efficiency IE (%) of MPIP. Analysis of the data reveals that the increase in inhibition efficiency with rising MPIP concentration is attributed to the adsorption of the inhibitor onto the aluminum surface. This adsorption is facilitated by the availability of non-bonding electron pairs on heteroatoms (N and O) and the π-electrons of the aromatic rings, enabling chemisorptive interactions with the metal surface. Such interactions result in the formation of a dense and stable adsorbed film, which acts as a physical barrier that limits the access of aggressive species to the metal surface, thereby reducing the anodic dissolution process.

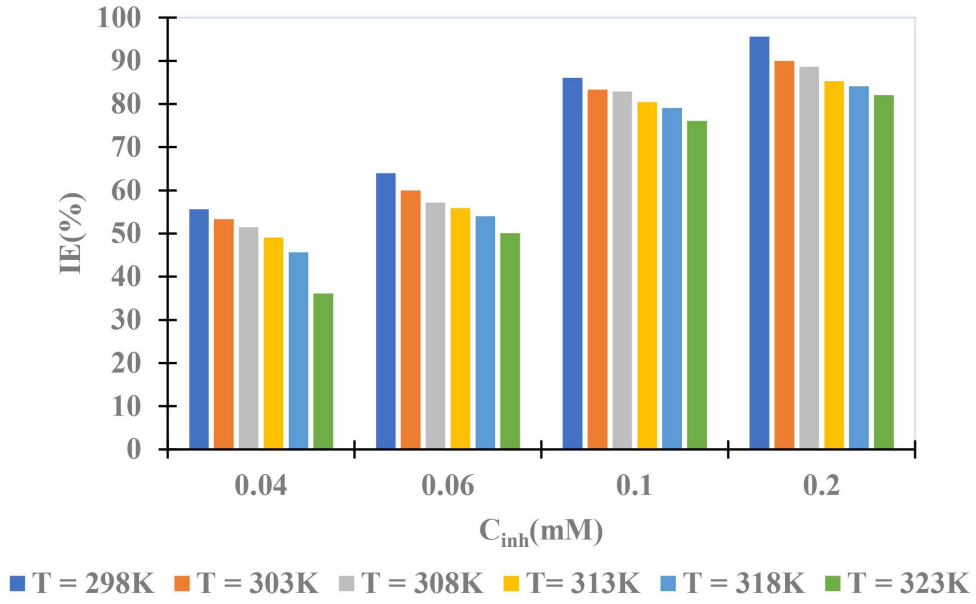

Figure 3. Inhibition efficiency vs. temperature for different concentrations in MPIP.

However, a decrease in inhibition efficiency is observed with increasing temperature. This behavior is ascribed to the thermal desorption of MPIP, which occurs due to increased thermal agitation and reduced stability of the inhibitor–metal interactions. The acceleration of desorption at elevated temperatures compromises the integrity of the protective film, thereby exposing the metal surface to corrosive attack. This temperature-dependent behavior aligns with findings reported by [41] [42], and suggests a predominantly physico-chemical adsorption mechanism that is sensitive to the thermdynamic conditions of the system.

3.2. Adsorption Isotherm and Thermodynamic Considerations

3.2.1. Adsorption Isotherms and Thermodynamic Parameters

A thermodynamic study was carried out to determine the nature and mechanism of adsorption of the inhibitor on the aluminum surface.

It is widely acknowledged that adsorption isotherms provide useful insights into the mechanism of corrosion inhibition. In order to obtain the isotherm type model, one supposes that inhibitor acts via a simple adsorption mode. Thus, the apparent corrosion rate of the inhibited aluminum sample is proportional to the ratio of the surface covered θ and that not covered $1-\theta$ by the inhibitor. Fractional coverage values θ have been evaluated for different concentrations of the compound under study from corrosion rates in uninhibited and inhibited solutions by means of Equation (2).

Five isotherm models have been explored to describe phenomena at the metal/solution interface. The aim of this approach is to assess the compound's adsorption capacity, elucidate the inhibition mechanism involved and optimize the process. So we have retained Langmuir, Temkin, Frumkin, El-Awady and Adejo-Ekwenchi isotherms [43]-[47]. The Equations that define these isotherms are expressed in Table 1.

Table 1. Equations of studied isotherms.

Isotherm	Equations	
Langmuir	$\frac{C_{inh}}{\theta}=\frac{1}{K_{ads}}+C_{inh}$	(12)
Temkin	$\theta=\frac{2.303}{f}\left(\log K_{ads}+\log C_{inh}\right)$	(13)
El-Awady	$\log\left(\frac{\theta}{1-\theta}\right)=\log K'+y\log C_{inh}$	(14)
Frumkin	$\log\left[\theta(1-\theta)C_{inh}\right]=\log K_{ads}+2f\theta$	(15)
Adejo-Ekwenchi	$\log\left(\frac{1}{1-\theta}\right)=\log K_{AE}+b\log C_{inh}$	(16)

C_{inh} is MPIP's concentration;
K_{ads} is the equilibrium constant of the adsorption process;
f is a factor energetic inhomogeneity in the surface;
θ is surface coverage;
$K_{ads}=K'^{1/y}$; $1/y$ is active sites occupied by an inhibitor molecule;
K_{AE}, b are d'Adejo-Ekwenchi isotherm parameters.

Figures 4-8 illustrate the best fit obtained from the plot of fractional surface coverage θ versus C_{inh}. All the tested isotherms yield straight lines as shown in Figures 4-8. Table 2 gives the different parameters of studied isotherms.

Langmuir isotherm exhibited the highest determination coefficients (values close to 1), indicating excellent agreement with the experimental results. This model assumes monolayer adsorption on a homogeneous surface without interactions between adsorbed molecules. The slopes of the Langmuir plots were close to unity,

confirming the applicability of this model and suggesting that the MPIP molecules adsorb uniformly across the aluminum surface, with negligible lateral interactions [48].

Temkin isotherm accounted for weak interactions between adsorbed species and suggested slight heterogeneity in adsorption energies. Although its fit was slightly less accurate than Langmuir's, it remains relevant, especially at higher inhibitor concentrations [49].

While El-Awady model proposed heterogeneous adsorption sites and potential molecular interactions. Its R^2 values were close to unity but still lower than those of the Langmuir model, indicating minor surface heterogeneity or intermolecular effects [46].

The Frumkin isotherm, an extension of the Langmuir model, incorporates attractive or repulsive interactions between adsorbed molecules. The model showed a good fit ($R^2 \approx 1$) and suggested the presence of weak electrostatic forces. This supports the idea of physical adsorption contributing to the inhibitory process [50].

Finally, the Adejo-Ekwenchi isotherm also fitted the experimental data well. The decreasing trend of the slope parameter b with increasing temperature, as observed in **Table 2**, points toward a physisorption mechanism. According to [42] [48] [51], such behavior is characteristic of van der Waals-type interactions, which do not involve the formation of chemical bonds and are easily reversed at elevated temperatures.

Overall, the Langmuir model remains the most suitable under the tested conditions. However, the inclusion of other isotherms provides complementary insight into the nature of the adsorption process, including molecular interactions, surface heterogeneity, and thermally sensitive physical adsorption mechanisms.

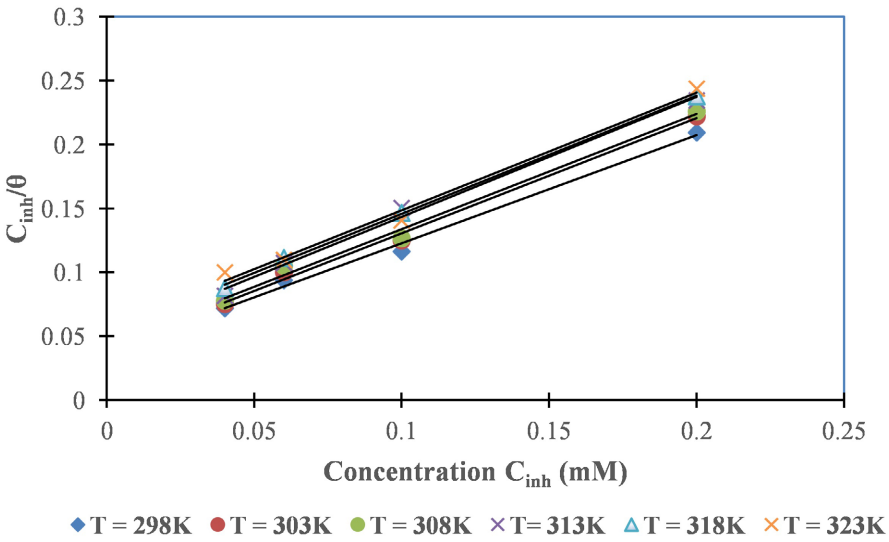

Figure 4. Langmuir adsorption isotherms for inhibition of aluminum corrosion in 1.0 M HCl by different concentrations of MPIP at temperatures 298 K to 308 K.

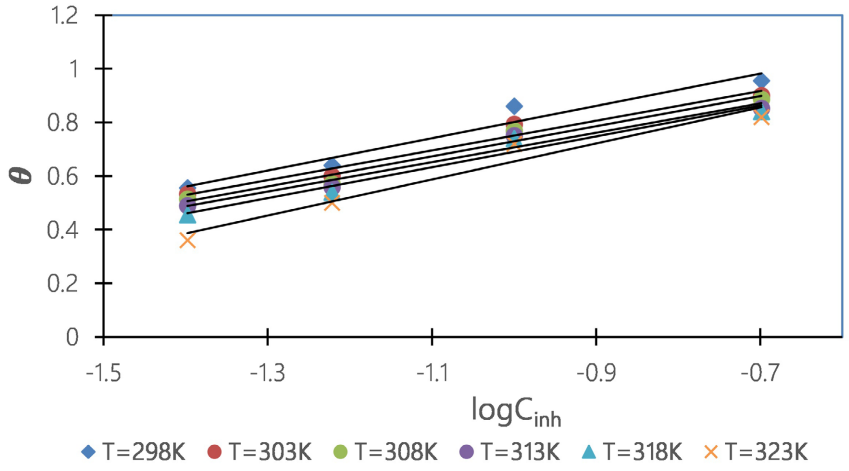

Figure 5. Temkin adsorption isotherms for inhibition of aluminum corrosion in 1.0 M HCl by different concentrations of MPIP at temperatures 298 K to 323 K.

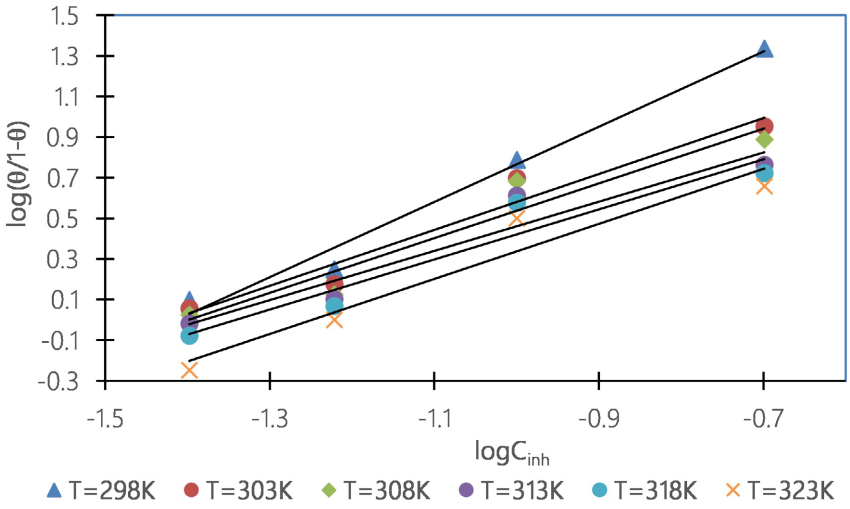

Figure 6. El-Awady adsorption isotherms for inhibition of aluminum corrosion in 1.0 M HCl by different concentrations of MPIP at temperatures 298 K to 323 K.

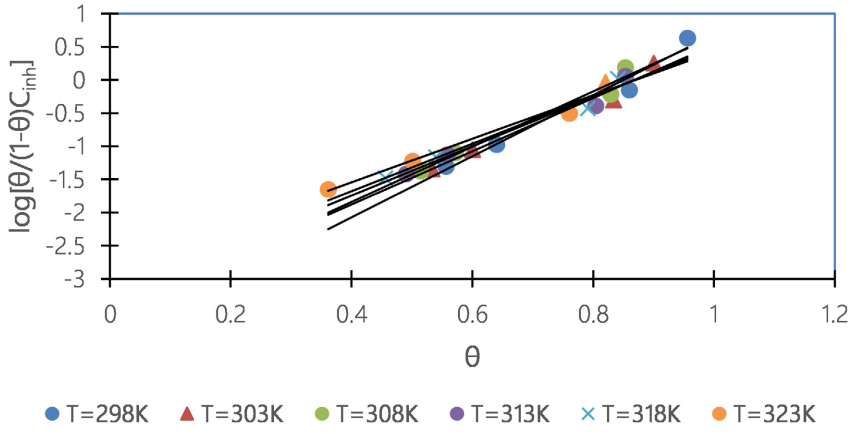

Figure 7. Frumkin adsorption isotherms for inhibition of aluminum corrosion in 1.0 M HCl by different concentrations of MPIP at temperatures 298 K to 323 K.

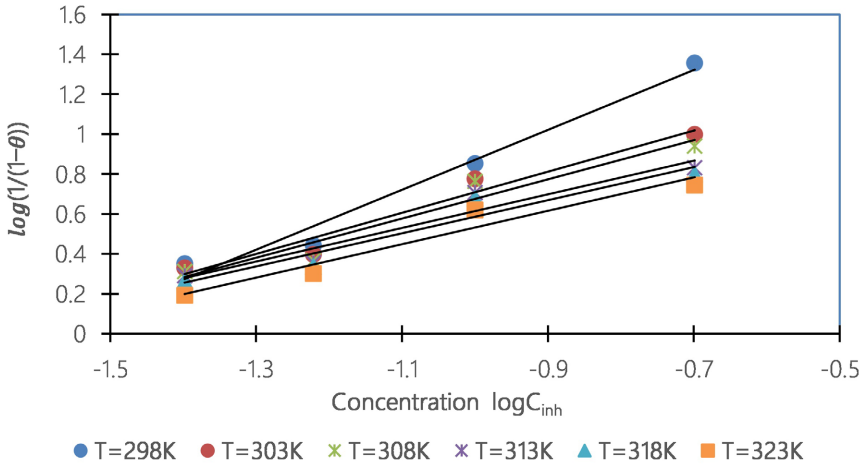

Figure 8. Adejo-Ekwenchi adsorption isotherms for inhibition of aluminum corrosion in 1.0 M HCl by different concentrations of MPIP at temperatures 298 K to 323 K.

Table 2. Parameters deduced from other adsorption isotherms using results reported for MPIP.

Isotherm	T(K)	R^2	Slope	Intercept
Langmuir	298	0.9937	0.8457	0.0382
	303	0.9947	0.9028	0.0403
	308	0.9912	0.9022	0.0421
	313	0.9933	0.9380	0.0497
	318	0.9990	0.9258	0.0532
	323	0.9905	0.9203	0.0565
Temkin	298	0.9525	0.6033	1.4044
	303	0.9663	0.5529	1.3037
	308	0.9678	0.5629	1.2927
	313	0.9650	0.5465	1.2532
	318	0.9618	0.5768	1.2672
	323	0.9510	0.6728	1.3272
El-Awady	298	0.9827	1.8521	2.6179
	303	0.9519	1.3766	1.9581
	308	0.9289	1.3470	1.8851
	313	0.9196	1.2109	1.6728
	318	0.9212	1.2315	1.6531
	323	0.9301	1.3550	1.6918
Frumkin	298	0.9718	4.5990	−3.9093
	303	0.9724	4.0166	−3.4864
	308	0.9717	4.1649	−3.5039
	313	0.9724	3.7244	−3.2337
	318	0.9738	3.5804	−3.1083
	323	0.9773	3.2825	−3.8586

Continued

Adejo-Ekwenchi	298	0.9737	1.5001	2.3713
	303	0.957	1.0294	1.7382
	308	0.9362	0.9808	1.6564
	313	0.9266	0.8420	1.4561
	318	0.9287	0.8289	1.4148
	323	0.9441	0.8374	1.3699

3.2.2. Effect of Temperature

The study of adsorption isotherms serves as a fundamental tool for elucidating the molecular-level mechanisms governing corrosion inhibition. A better understanding of the adsorption behaviour of an inhibitor can be achieved by investigating the thermodynamics of the adsorption process. Thus, the thermodynamic properties are based on the analysis of adsorption thermodynamic parameters. The standard free energy of adsorption (ΔG_{ads}^{0}) is calculated using the following Equation [50]:

$$\Delta G_{ads}^{0} = -RT\ln\left(55.5K_{ads}\right) \tag{17}$$

where:

- 55.5 is the molar concentration of water in the corrosive solution (in mol·L^{-1}),
- R is the universal gas constant, and T is the absolute temperature in Kelvin,
- K_{ads} is the adsorption equilibrium constant, which is determined from the intercept of the linearized Langmuir adsorption isotherm plots ($1/K_{ads}$ corresponds to the y-intercept; see Table 2.

Indeed, the adsorption of MPIP on the aluminum surface follows the Langmuir isotherm model most appropriately.

Furthermore, the standard enthalpy change of adsorption (ΔH_{ads}^{0}) and the standard entropy change of adsorption (ΔS_{ads}^{0}) are determined from the Gibbs-Helmholtz Equation:

$$\Delta G_{ads}^{0} = \Delta H_{ads}^{0} - T\Delta S_{ads}^{0} \tag{18}$$

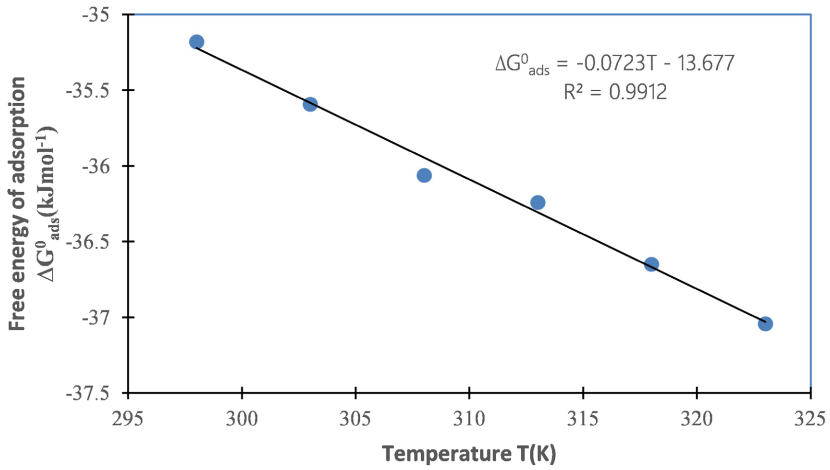

Figure 9. ΔG_{ads} versus temperature.

In fact, plotting ΔG_{ads}^{0} as a function of temperature (Figure 9) allows for the determination of the thermodynamic quantities ΔH_{ads}^{0} and ΔS_{ads}^{0}. The corresponding values derived from this analysis are summarized in Table 3.

Table 3. K_{ads} and thermodynamic adsorption parameters for MPIP.

T (K)	K_{ads}	ΔG_{ads}^{0} (kJ·mol^{-1})	ΔH_{ads}^{0} (kJ·mol^{-1})	ΔS_{ads}^{0} (J·mol^{-1}·K^{-1})
298	26178.01047	−35.179783	−13.677	72.3
303	24813.89578	−35.59230554		
308	23866.34845	−36.07998561		
313	20120.72435	−36.22165414		
318	18867.92453	−36.63039133		
323	17857.14286	−37.05855328		

The negative values of the standard Gibbs free energy of adsorption (ΔG_{ads}^{0}) indicate that the adsorption of MPIP onto the aluminum surface is a spontaneous process, accompanied by the formation of a stable adsorbed layer [52]. The measured values, ranging from −35 to −37 kJ·mol^{-1}, suggest that a mixed adsorption mode, so the mechanism likely involves both physisorption and some degree of chemisorption [51].

Furthermore, the standard enthalpy change of adsorption (ΔH_{ads}^{0}) is negative, confirming that the process is exothermic [40]. This exothermic nature favors physisorption, although it is often associated with a decrease in inhibition efficiency at elevated temperatures.

Finally, the positive value of the standard entropy change of adsorption (ΔS_{ads}^{0}) reflects an increase in disorder at the metal/solution interface during MPIP adsorption. This increase is primarily attributed to the displacement of water molecules initially adsorbed on the aluminum surface, which are replaced by inhibitor molecules [30]-[33] [40].

The effect of temperature on corrosion and its inhibition process for aluminum in 1 M HCl in absence and presence of different concentrations of MPIP at different temperatures ranging from 298 K to 323 K was evaluated. The dependence of corrosion rate on the temperature can be regarded as an Arrhenius-type process, the rate of which is given by Arrhenius:

$$\log W = \log A - \frac{E_a}{2.3RT} \tag{19}$$

where W is the corrosion rate in the presence of inhibitor, E_a the apparent activation energy, R the universal gas constant, A the frequency factor.

Corrosion rates were used to additionally achieve data on the apparent activation enthalpy (ΔH_a^*) and activation entropy (ΔS_a^*) changes for the formation of the activated complex in the transition state using the relation (20):

$$\log\left(\frac{W}{T}\right) = \log\left(\frac{R}{\aleph h}\right) + \frac{\Delta S_a^*}{2.303R} - \frac{\Delta H_a^*}{2.303RT} \tag{20}$$

where h is Planck's constant and N is Avogadro number.

The plots of $\log W$ and $\log W/T$ versus $1/T$ for aluminum in corrosive environment in the absence and in the presence of various concentrations of the MPIP inhibtor are given by Figure 10 and Figure 11.

The slopes $\frac{E_a}{2.3RT}$ and $\frac{\Delta H_a^*}{2.303RT}$ of the straight lines were used to evaluate (E_a) and (ΔH_a^*), whereas the intercept $\log\left(\frac{R}{\aleph h}\right)+\frac{\Delta S_a^*}{2.303R}$ was used to evaluate (ΔS_a^*). All the results are presented in Table 4.

The value of activation energy (E_a) for hydrochloric acid solution without MPIP is 98.52 kJ/mol, while in the presence of MPIP as a corrosion inhibitor is 111.54 kJ/mol. The high activation energy value of MPIP is often interpreted as suggesting the formation of a physical/electrostatic adsorption film [48].

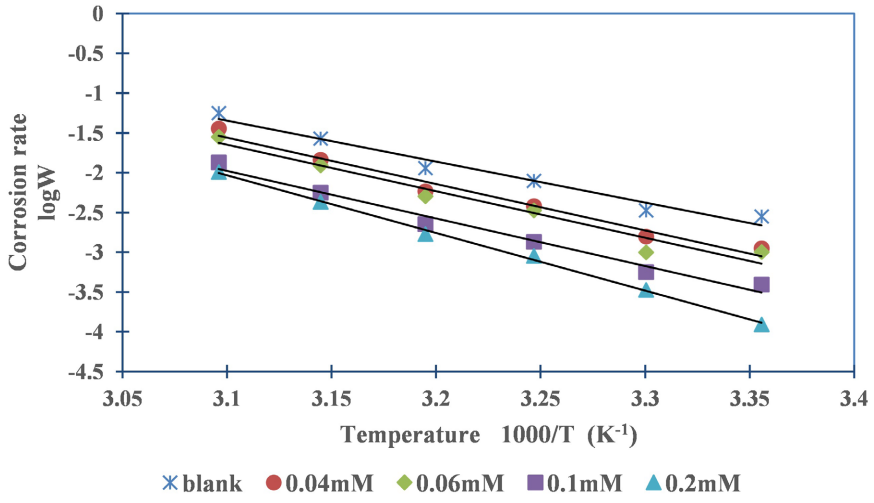

Figure 10. Arrhenius plots for aluminum in 1 M HCl without and with MPIP.

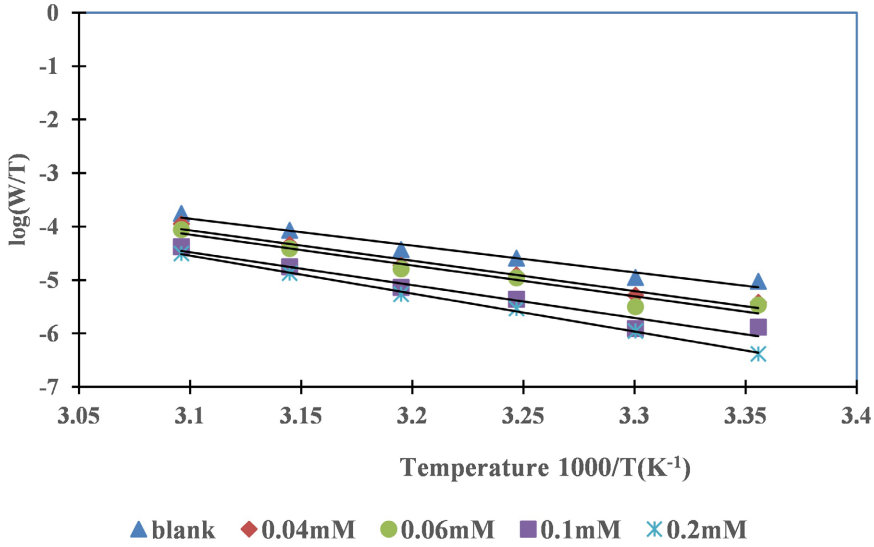

Figure 11. Arrhenius plots for aluminum in 1 M HCl without and with MPIP.

The positive ΔH_a^* value refers to an endothermic dissolution process for surface of aluminum at room temperature in the presence of MPIP molecules [53]. ΔH_a^* increased with a temperature increase, which supports the endothermic nature of aluminum surface dissolution and the decrease of the inhibition performance of MPIP molecules. The apparent entropy activation (ΔS_a^*) values at room temperature

were positive with increasing temperature. In the absence of MPIP molecules, the apparent entropy activation values were also positive at higher concentrations of MPIP. (ΔS_a^*) with considerable and positive values implies that the activated complex in the rate-determining step means a dissociation rather than an association stage, suggesting that an increase in disordering takes place on proceeding from reactants to the activated complex [54].

Table 4. Kinetic parameters for aluminum in 1.0 M HCl in the presence and absence of MPIP.

Concentration mM	E_a (kJ·mol^{-1})	ΔH_a^* (kJ·mol^{-1})	ΔS_a^* (J·mol^{-1}·K^{-1})
blank	98.51990803	95.93892672	25.795328
0.04	111.5416964	108.9607151	61.981504
0.06	112.1490989	110.1965971	64.182144
0.1	114.5480511	117.6118886	80.926144
0.2	138.5950559	136.0140746	136.688448

3.3. Quantum Chemical Calculations

3.3.1. Global Reactivity

Quantum chemical principles have been widely used to study corrosion inhibition including structure optimization calculations, semi-empirical, ab initio and DFT calculations. To corroborate the experimental results and the electronic parameters which are very important to explain the molecule reactivity, a computational analysis based on density functional theory (DFT) was carried out.

The quantum chemical parameters for the neutral form (**Figure 12**) of the investigated inhibitor calculated by DFT/B3LYP with the 6-31G (d, p) are listed in **Table 5**. The values of the frontier molecular orbital energies (*i.e.* energy of the highest occupied molecular orbital (E_{HOMO}), energy of the lowest unoccupied molecular orbital (E_{LUMO}), the energy gap (ΔE_{L-H}), total energy (E_T), Hardness (η), Electrophilicity (ω), Ionization Potential (I), and dipole moment (μ) were also calculated [46].

Generally, the energy gap of a molecule is a quantum chemical parameter that indicates hardness or softness of molecular species. Hard molecules are characterized with larger value of energy gap and are less reactive than soft molecules, which are characterize by small energy gap [55]. The quantum chemical parameters of MPIP provide consistent evidence for its strong inhibitory performance on aluminum. The relatively high HOMO energy indicates that MPIP can readily donate electrons to the metal surface, while its low LUMO energy suggests a simultaneous

ability to accept electrons, thereby favoring donor–acceptor interactions [42] [56]-[58]. This dual behavior, combined with the small energy gap (ΔE), reflects high chemical reactivity and facilitates electron transfer during adsorption. The moderate dipole moment (μ = 1.8126 D) confirms sufficient molecular polarity to promote surface interactions. In addition, the high softness (σ) and low hardness (η) values classify MPIP as a "soft" molecule, further enhancing its adsorption affinity. The elevated electrophilicity index (ω = 3.6942) highlights its strong electron-accepting tendency, particularly toward reactive species such as H^+ in acidic media, supporting the formation of a protective barrier layer on the aluminum surface. Moreover, the lower electronegativity of MPIP (χ_{inh} = 3.7542 eV) compared to aluminum (χ_{Al} = 4.28 eV), along with the positive fraction of electrons transferred ($\Delta N > 0$), confirms electron migration from the metal to the inhibitor [58]. Taken together, these descriptors underline the capability of MPIP to strongly adsorb onto aluminum through synergistic donor–acceptor and electrostatic interactions, thereby ensuring effective corrosion inhibition.

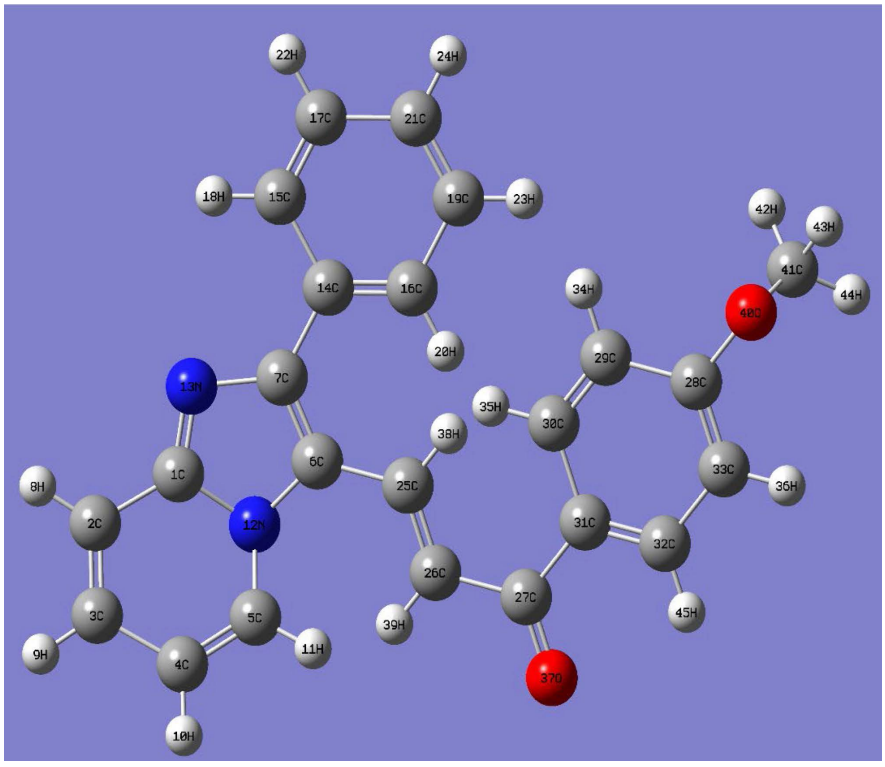

Figure 12. Optimized structure of MPIP.

Table 5. Theoretical properties of MPIP calculated using DFT at the B3LYP/6-31G (d) basis set.

Parameters	MPIP
E_{HOMO} (eV)	−5.6617
E_{LUMO} (eV)	−1.8466
Energy gap ΔE_{L-H}	3.8151

Continued

Dipole moment μ (D)	1.8126
Ionization energy (eV)	5.6617
Electron affinity A (eV)	1.8466
Absolute electronegativity χ (eV)	3.7542
Hardness η (eV)	1.9076
Softness σ (eV)$^{-1}$	0.5242
Fraction of electron transferred ΔN	0.3213
Electrophylicity index ω	3.6942
Total energy E_T (Ha)	−1146.9877

3.3.2. Local Reactivity

Reactive sites correspond to molecular regions that are most likely to donate or accept electrons in interactions with the metal. In the case of MPIP, the molecule tends to accept electrons through the LUMO and to donate electrons via the HOMO (**Figure 13**). The identification of these sites is based on the analysis of Fukui functions (f_k^+ , f_k^-) and the dual descriptor ($\Delta f_k(r)$) [59]. According to the literature, the atom with the highest values of f_k^+ and $\Delta f_k(r)$ is considered the most favorable site for nucleophilic attack, generally associated with the LUMO of MPIP. Conversely, the atom displaying the highest f_k^- value and the lowest $\Delta f_k(r)$ is the predominant site for electrophilic attack, which is linked to the HOMO [57] [60].

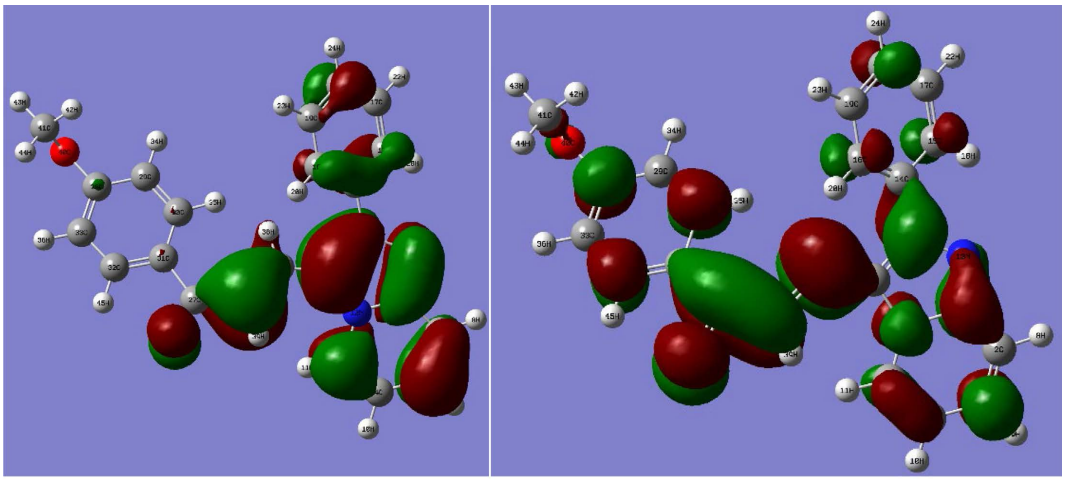

HOMO LUMO

Figure 13. HOMO and LUMO orbitals of studied molecule.

The Fukui function analysis in **Table 6** provides further insight into the reactive sites of MPIP and their role in its adsorption on aluminum. Carbon C (1) was identified as the most favorable site for electrophilic attack, while oxygen O (37) emerged as the primary nucleophilic center.

Table 6. Local MPIP reactivity sites.

Atoms	$q_k(N+1)$	$q_k(N)$	$q_k(N-1)$	f_k^+	f_k^-	$\Delta f_k(r)$
1 C	0.084159	0.454511	0.058647	−0.370352	**0.395864**	**−0.766216**
2 C	−0.028102	−0.080094	−0.027294	0.051992	−0.0528	0.104792
3 C	0.112039	−0.08167	0.060065	0.193709	−0.141735	0.335444
4 C	−0.046961	−0.131366	−0.015956	0.084405	−0.11541	0.199815
5 C	0.078677	0.094616	0.021482	−0.015939	0.073134	−0.089073
6 C	0.354291	0.202057	0.017848	0.152234	0.184209	−0.031975
7 C	0.061676	0.121785	0.083259	−0.060109	0.038526	−0.098635
8 H	0.00172	0.120028	0.001061	−0.118308	0.118967	−0.237275
9 H	−0.004834	0.106999	−0.003117	−0.111833	0.110116	−0.221949
10 H	0.002723	0.107294	0.000418	−0.104571	0.106876	−0.211447
11 H	−0.002131	0.131794	−0.00119	−0.133925	0.132984	−0.266909
12 N	−0.040292	−0.52734	0.040049	0.487048	−0.567389	1.054437
13 N	0.026409	−0.544625	−0.038577	0.571034	−0.506048	1.077082
14 C	0.039551	0.075921	0.011597	−0.03637	0.064324	−0.100694
15 C	0.020128	−0.085454	−0.000649	0.105582	−0.084805	0.190387
16 C	0.114824	−0.080355	0.062354	0.195179	−0.142709	0.337888
17 C	−0.020175	−0.095429	0.00634	0.075254	−0.101769	0.177023
18 H	−0.001103	0.117649	−0.000008	−0.118752	0.117657	−0.236409
19 C	−0.040889	−0.096489	−0.020198	0.0556	−0.076291	0.131891
20 H	−0.005708	0.03079	0.011379	−0.036498	0.019411	−0.055909
21 C	0.121782	−0.092642	0.036204	0.214424	−0.128846	0.34327
22 H	0.000487	0.096181	−0.000524	−0.095694	0.096705	−0.192399
23 H	0.001044	0.090707	0.00052	−0.089663	0.090187	−0.17985
24 H	−0.005068	0.092197	−0.001853	−0.097265	0.09405	−0.191315
25 C	−0.11745	0.056877	0.153823	−0.174327	−0.096946	−0.077381
26 C	0.248923	−0.167263	0.113671	0.416186	−0.280934	0.69712
27 C	−0.042584	0.370791	0.107162	−0.413375	0.263629	−0.677004
28 C	0.008467	0.334024	0.060823	−0.325557	0.273201	−0.598758
29 C	−0.004117	−0.154673	−0.026183	0.150556	−0.12849	0.279046
30 C	0.008602	0.035121	0.030289	−0.026519	0.004832	−0.031351
31 C	0.017028	0.042398	0.002711	−0.02537	0.039687	−0.065057
32 C	−0.011232	−0.128044	0.066876	0.116812	−0.19492	0.311732
33 C	0.018728	−0.114015	−0.020282	0.132743	−0.093733	0.226476
34 H	0.000022	0.092786	0.000798	−0.092764	0.091988	−0.184752
35 H	−0.001119	0.022979	0.00695	−0.024098	0.016029	−0.040127
36 H	−0.000782	0.103264	0.000598	−0.104046	0.102666	−0.206712

Continued

37 O	0.051396	−0.498977	0.220816	**0.550373**	−0.719793	**1.270166**
38 H	0.007076	0.007882	−0.010492	−0.000806	0.018374	−0.01918
39 H	−0.009184	0.111216	−0.006734	−0.1204	0.11795	−0.23835
40 O	0.001172	−0.530633	−0.001501	0.531805	−0.529132	1.060937
41 C	0.000491	−0.119387	0.001422	0.119878	−0.120809	0.240687
42 H	0.000004	0.120512	−0.000028	−0.120508	0.12054	−0.241048
43 H	0.0001	0.134414	0.000992	−0.134314	0.133422	−0.267736
44 H	−0.00004	0.123414	0.000005	−0.123454	0.123409	−0.246863
45 H	0.000254	0.130249	−0.003574	−0.129995	0.133823	−0.263818

These findings indicate that electron transfer to the metal occurs predominantly through C (1), whereas O (37) facilitates nucleophilic interactions by generating local electron deficiencies (Figure 14). Such donor–acceptor exchanges reinforce the inhibitor–metal bonding and contribute to the formation of a stable Al–MPIP protective layer. This electronic distribution strongly supports the adsorption capacity of MPIP and its effectiveness in preventing aluminum dissolution in aggressive media, in agreement with previous studies [57] [60].

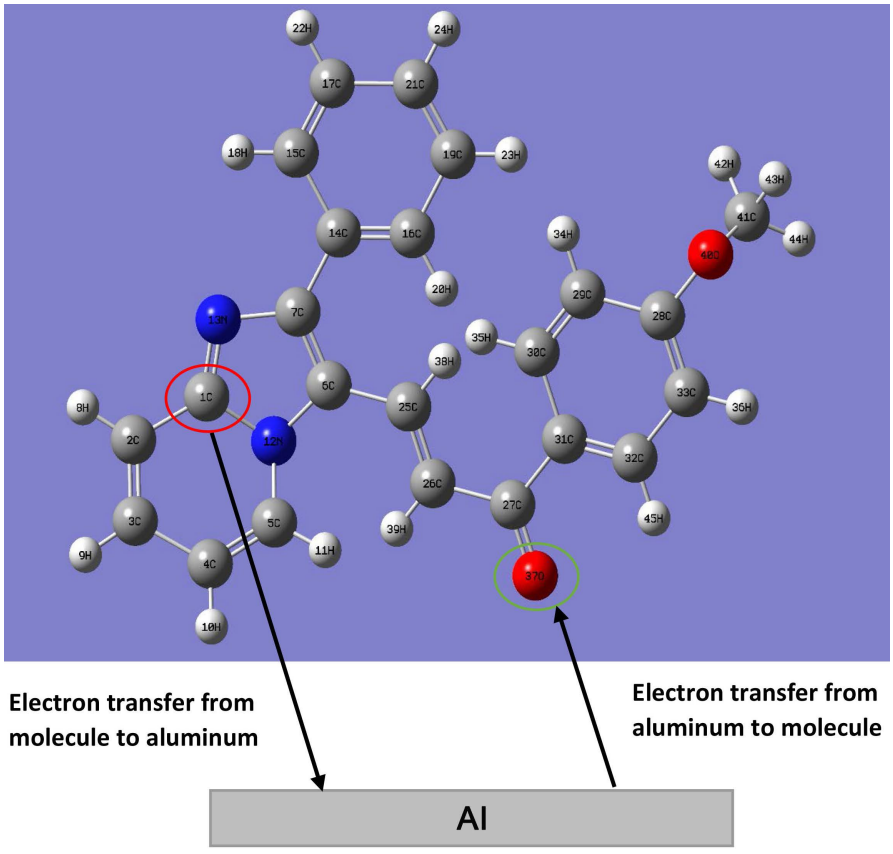

Figure 14. Electron exchange between the molecule and aluminum.

4. Conclusion

This study investigated the adsorption and corrosion inhibition behavior of (2E)-1-(4-methoxyphenyl)-3-(2-phenylH-imidazo [1, 2-*a*] pyridine-3-yl) prop-2-en-1-one on aluminum in 1 M HCl. Gravimetric tests demonstrated that the compound exhibits significant inhibition efficiency, which increases with concentration and decreases with temperature. Adsorption follows the Langmuir model, indicating monolayer physisorption primarily driven by van der Waals interactions. Thermodynamic analysis revealed that adsorption is spontaneous, exothermic, and accompanied by increased entropy. DFT calculations and local reactivity analysis identified carbon C (1) and oxygen O (37) as key active sites, confirming the molecule's ability to transfer electrons to and from the metal surface. These interactions enhance adsorption, forming a protective barrier that effectively reduces aluminum dissolution. Theoretical predictions align closely with experimental observations, supporting the compound's potential as an effective corrosion inhibitor at low temperatures.

Conflicts of Interest

The authors declare no conflicts of interest regarding the publication of this paper.

References

[1] Cramer, S.D. and Covino Jr., B.S. (2003) Corrosion: Fundamentals, Testing, and Protection, Volume 13A, ASM Handbook. *Journal of Thermal Spray Technology*, **12**, 459-463.

[2] Ahmed, M.A., Amin, S. and Mohamed, A.A. (2024) Current and Emerging Trends of Inorganic, Organic and Eco-Friendly Corrosion Inhibitors. *RSC Advances*, **14**, 31877-31920. https://doi.org/10.1039/d4ra05662k

[3] El-Maksoud, S.A.A., Migahed, M.A., Gouda, M.M. and El-Dossoki, F.I. (2025) Novel Gemini Cationic Thiazole-Based Surfactants as Carbon Steel Corrosion Inhibitors in 1 M HCl Using Experimental and Theoretical Tools. *Scientific Reports*, **15**, Article No. 17512. https://doi.org/10.1038/s41598-025-02173-x

[4] Zaafarany, I.A. (2013) Corrosion Inhibition of Mild Steel in Hydrochloric Acid Solution Using Cationic Surfactant Olyel-Amido Derivatives. *International Journal of Electrochemical Science*, **8**, 9531-9542. https://doi.org/10.1016/s1452-3981(23)12991-9

[5] Shenoy, P., Kedimar, N. and Rao, S.A. (2024) A Comprehensive Review on Anticorrosive Behaviour of Surfactants across Diverse Metals Using Multiple Techniques: Current Insights and Future Horizons. *Chemical Engineering Journal Advances*, **20**, Article ID: 100645. https://doi.org/10.1016/j.ceja.2024.100645

[6] Al-Amiery, A.A., Binti Kassim, F.A., Kadhum, A.A.H. and Mohamad, A.B. (2016) Synthesis and Characterization of a Novel Eco-Friendly Corrosion Inhibition for Mild Steel in 1 M Hydrochloric Acid. *Scientific Reports*, **6**, Article No. 19890. https://doi.org/10.1038/srep19890

[7] Pourmohseni, M., Rashidi, A. and Karimkhani, M. (2024) Preparation of Corrosion Inhibitor from Natural Plant for Mild Stil Immersed in an Acidic Environmental: Experimental and Theoretical Study. *Scientific Reports*, **14**, Article No. 7937.

https://doi.org/10.1038/s41598-024-58637-z

[8] Kadhim, A., Al-Okbi, A.K., Jamil, D.M., Qussay, A., Al-Amiery, A.A., Gaaz, T.S., *et al.* (2017) Experimental and Theoretical Studies of Benzoxazines Corrosion Inhibitors. *Results in Physics*, **7**, 4013-4019. https://doi.org/10.1016/j.rinp.2017.10.027

[9] Yadav, M., Gope, L. and Sarkar, T.K. (2016) Synthesized Amino Acid Compounds as Eco-Friendly Corrosion Inhibitors for Mild Steel in Hydrochloric Acid Solution: Electrochemical and Quantum Studies. *Research on Chemical Intermediates*, **42**, 2641-2660. https://doi.org/10.1007/s11164-015-2172-5

[10] Goyal, M., Kumar, S., Bahadur, I., Verma, C. and Ebenso, E.E. (2018) Organic Corrosion Inhibitors for Industrial Cleaning of Ferrous and Non-Ferrous Metals in Acidic Solutions: A Review. *Journal of Molecular Liquids*, **256**, 565-573. https://doi.org/10.1016/j.molliq.2018.02.045

[11] Verma, C., Haque, J., Quraishi, M.A. and Ebenso, E.E. (2019) Aqueous Phase Environmental Friendly Organic Corrosion Inhibitors Derived from One Step Multicomponent Reactions: A Review. *Journal of Molecular Liquids*, **275**, 18-40. https://doi.org/10.1016/j.molliq.2018.11.040

[12] Wei, H., Heidarshenas, B., Zhou, L., Hussain, G., Li, Q. and Ostrikov, K. (2020) Green Inhibitors for Steel Corrosion in Acidic Environment: State of Art. *Materials Today Sustainability*, **10**, Article ID: 100044. https://doi.org/10.1016/j.mtsust.2020.100044

[13] Umoren, S.A., Solomon, M.M., Madhankumar, A. and Obot, I.B. (2020) Exploration of Natural Polymers for Use as Green Corrosion Inhibitors for AZ31 Magnesium Alloy in Saline Environment. *Carbohydrate Polymers*, **230**, Article ID: 115466. https://doi.org/10.1016/j.carbpol.2019.115466

[14] Murmu, M., Saha, S.K., Murmu, N.C. and Banerjee, P. (2022) Nitrate as Corrosion Inhibitor. In: Verma, C., Aslam, J. and Hussain, C.M., Eds., *Inorganic Anticorrosive Materials*, Elsevier, 269-296. https://doi.org/10.1016/b978-0-323-90410-0.00015-5

[15] De Ketelaere, E., Moed, D., Vanoppen, M., Verliefde, A.R.D., Verbeken, K. and Depover, T. (2023) Sodium Silicate Corrosion Inhibition Behaviour for Carbon Steel in a Dynamic Salt Water Environment. *Corrosion Science*, **217**, Article ID: 111119. https://doi.org/10.1016/j.corsci.2023.111119

[16] Machado Fernandes, C., Faro, L.V., Pina, V.G.S.S., de Souza, M.C.B.V., Boechat, F.C.S., de Souza, M.C., *et al.* (2020) Study of Three New Halogenated Oxoquinolinecarbohydrazide N-Phosphonate Derivatives as Corrosion Inhibitor for Mild Steel in Acid Environment. *Surfaces and Interfaces*, **21**, Article ID: 100773. https://doi.org/10.1016/j.surfin.2020.100773

[17] Anaee, R.A.M. (2013) Sodium Silicate and Phosphate as Corrosion Inhibitors for Mild Steel in Simulated Cooling Water System. *Arabian Journal for Science and Engineering*, **39**, 153-162. https://doi.org/10.1007/s13369-013-0865-x

[18] Desai, P.D., Pawar, C.B., Avhad, M.S. and More, A.P. (2022) Corrosion Inhibitors for Carbon Steel: A Review. *Vietnam Journal of Chemistry*, **61**, 15-42. https://doi.org/10.1002/vjch.202200111

[19] Haque, J., Srivastava, V., Verma, C. and Quraishi, M.A. (2017) Experimental and Quantum Chemical Analysis of 2-Amino-3-((4-((S)-2-Amino-2-Carboxyethyl)-1h-Imidazol-2-Yl)thio) Propionic Acid as New and Green Corrosion Inhibitor for Mild Steel in 1 M Hydrochloric Acid Solution. *Journal of Molecular Liquids*, **225**, 848-855. https://doi.org/10.1016/j.molliq.2016.11.011

[20] Ahmed, M.A., Ahmed, M.A. and Mohamed, A.A. (2023) Adsorptive Removal of Tetracycline Antibiotic onto Magnetic Graphene Oxide Nanocomposite Modified with

Polyvinylpyrroilidone. *Reactive and Functional Polymers*, **191**, Article ID: 105701. https://doi.org/10.1016/j.reactfunctpolym.2023.105701

[21] Emregül, K.C., Kurtaran, R. and Atakol, O. (2003) An Investigation of Chloride-Substituted Schiff Bases as Corrosion Inhibitors for Steel. *Corrosion Science*, **45**, 2803-2817. https://doi.org/10.1016/s0010-938x(03)00103-3

[22] Hussein, R.K., Abou-Krisha, M. and Yousef, T.A. (2021) Theoretical and Experimental Studies of Different Amine Compounds as Corrosion Inhibitors for Aluminum in Hydrochloric Acid. *Biointerface Research in Applied Chemistry*, **11**, 9772. https://doi.org/10.33263/BRIAC112.97729785

[23] Belghiti, M.E., Nahlé, A., Ansari, A., Karzazi, Y., Tighadouini, S., El Ouadi, Y., *et al.* (2017) Inhibition Effect of E and Z Conformations of 2-Pyridinealdazine on Mild Steel Corrosion in Phosphoric Acid. *Anti-Corrosion Methods and Materials*, **64**, 23-35. https://doi.org/10.1108/acmm-11-2015-1594

[24] Zarrouk, A., Zarrok, H., Ramli, Y., Bouachrine, M., Hammouti, B., Sahibed-dine, A., *et al.* (2016) Inhibitive Properties, Adsorption and Theoretical Study of 3,7-Dimethyl-1-(prop-2-Yn-1-Yl)quinoxalin-2(1h)-One as Efficient Corrosion Inhibitor for Carbon Steel in Hydrochloric Acid Solution. *Journal of Molecular Liquids*, **222**, 239-252. https://doi.org/10.1016/j.molliq.2016.07.046

[25] Elyoussfi, A., Dafali, A., Elmsellem, H., Steli, H., Bouzian, Y., Cherrak, K., El Ouadi, Y., Zarrouk, A. and Hammouti, B. (2016) Adsorption and Corrosion Inhibition of New Synthesized Quinoline on Mild Steel in HCl and H_2SO_4 Solutions. *Journal of Materials and Environmental Science*, **7**, 3344-3352.

[26] Belghiti, M.E., Bouazama, S., Echihi, S., Mahsoune, A., Elmelouky, A., Dafali, A., *et al.* (2020) Understanding the Adsorption of Newly Benzylidene-Aniline Derivatives as a Corrosion Inhibitor for Carbon Steel in Hydrochloric Acid Solution: Experimental, DFT and Molecular Dynamic Simulation Studies. *Arabian Journal of Chemistry*, **13**, 1499-1519. https://doi.org/10.1016/j.arabjc.2017.12.003

[27] Alaoui, K., Dkhireche, N., Ebn Touhami, M. and El Kacimi, Y. (2020) Review of Application of Imidazole and Imidazole Derivatives as Corrosion Inhibitors of Metals. In: El Kacimi, Y., Kaya, S. and Touir, R., Eds., *New Challenges and Industrial Applications for Corrosion Prevention and Control*, IGI Global, 101-131. https://doi.org/10.4018/978-1-7998-2775-7.ch005

[28] El-Hajjaji, F., Messali, M., Martínez de Yuso, M.V., Rodríguez-Castellón, E., Almutairi, S., Bandosz, T.J., *et al.* (2019) Effect of 1-(3-Phenoxypropyl) Pyridazin-1-Ium Bromide on Steel Corrosion Inhibition in Acidic Medium. *Journal of Colloid and Interface Science*, **541**, 418-424. https://doi.org/10.1016/j.jcis.2019.01.113

[29] Rokia, T.H., Tigori, M.A., Koffi, A.A. and Niamien, P.M. (2024) Exploring the Anticorrosion Performance of 2-(((4-Chlorobenzyl) Thiol) Methyl)-1h-Benzo[d]imidazole on Aluminum in 1 M HNO_3. *Journal of Scientific Research*, **16**, 899-915. https://doi.org/10.3329/jsr.v16i3.72318

[30] Rokia, T.H., Tigori, M.A., Koffi, A.A. and Niamien, P.M. (2025) Reactivity Analyzing of Some Benzimidazole Derivatives in Inhibiting Aluminum Corrosion in Nitric Acid Solution. *American Journal of Chemistry*, **15**, 1-9.

[31] Elewady, G.Y., El-Said, I.A. and Fouda, A.S. (2008) Effect of Anions on the Corrosion Inhibition of Aluminum in HCl Using Ethyl Trimethyl Ammonium Bromide as Cationic Inhibitor. *International Journal of Electrochemical Science*, **3**, 644-655. https://doi.org/10.1016/s1452-3981(23)15550-7

[32] Nnabuk, E.O. and Awe, F. (2018) Experimental and Quantum Chemical Studies on Ethanol Extract of *Phyllanthus amarus* (EEPA) as a Green Corrosion Inhibitor for

Aluminum in 1 M HCl. *Portugaliae Electrochimica Acta*, **36**, 231-247. https://doi.org/10.4152/pea.201804231

[33] Chaubey, N., Singh, V.K., Savita, Quraishi, M.A. and Ebenso, E.E. (2015) Corrosion Inhibition of Aluminium Alloy in Alkaline Media by *Neolamarckia cadamba* Bark Extract as a Green Inhibitor. *International Journal of Electrochemical Science*, **10**, 504-518. https://doi.org/10.1016/s1452-3981(23)05009-5

[34] Rahmani, H., Alaoui, K.I., Emran, K.M., El Hallaoui, A., Taleb, M., El Hajji, S., *et al.* (2019) Experimental and DFT Investigation on the Corrosion Inhibition of Mild Steel by 1,2,3-Triazole Regioisomers in 1M Hydrochloric Acid Solution. *International Journal of Electrochemical Science*, **14**, 985-998. https://doi.org/10.20964/2019.01.80

[35] Douche, D., Elmsellem, H., Anouar, E.H., Guo, L., Hafez, B., Tüzün, B., *et al.* (2020) Anti-Corrosion Performance of 8-Hydroxyquinoline Derivatives for Mild Steel in Acidic Medium: Gravimetric, Electrochemical, DFT and Molecular Dynamics Simulation Investigations. *Journal of Molecular Liquids*, **308**, Article ID: 113042. https://doi.org/10.1016/j.molliq.2020.113042

[36] Guo, L., Kaya, S., Obot, I.B., Zheng, X. and Qiang, Y. (2017) Toward Understanding the Anticorrosive Mechanism of Some Thiourea Derivatives for Carbon Steel Corrosion: A Combined DFT and Molecular Dynamics Investigation. *Journal of Colloid and Interface Science*, **506**, 478-485. https://doi.org/10.1016/j.jcis.2017.07.082

[37] Belghiti, M.E., Karzazi, Y., Dafali, A., Obot, I.B., Ebenso, E.E., Emran, K.M., *et al.* (2016) Anti-Corrosive Properties of 4-Amino-3,5-Bis(disubstituted)-1,2,4-Triazole Derivatives on Mild Steel Corrosion in 2 M H_3PO_4 Solution: Experimental and Theoretical Studies. *Journal of Molecular Liquids*, **216**, 874-886. https://doi.org/10.1016/j.molliq.2015.12.093

[38] Roque, J.M., Pandiyan, T., Cruz, J. and García-Ochoa, E. (2008) DFT and Electrochemical Studies of Tris(benzimidazole-2-Ylmethyl)amine as an Efficient Corrosion Inhibitor for Carbon Steel Surface. *Corrosion Science*, **50**, 614-624. https://doi.org/10.1016/j.corsci.2007.11.012

[39] Fukui, K., Yonezawa, T. and Shingu, H. (1952) A Molecular Orbital Theory of Reactivity in Aromatic Hydrocarbons. *The Journal of Chemical Physics*, **20**, 722-725. https://doi.org/10.1063/1.1700523

[40] Beda, R.H.B., Koffi, A.A., Ehouman, D., Niamien, P.M. and Trokourey, A. (2019) Theobromine as an Aluminium Corrosion Inhibitor in 1M HCL: Experimental and QSPR Studies. *Journal of Chemical and Pharmaceutical Research*, **11**, 73-91.

[41] Ibeji, C.U., Akintayo, D.C. and Adejoro, I.A. (2016) The Efficiency of Chloroquine as Corrosion Inhibitor for Aluminium in 1 M HCl Solution: Experimental and DFT Study. *Jordan Journal of Chemistry*, **11**, 38-49. https://doi.org/10.12816/0026487

[42] Yeo, M., Tigori, M.A., Cisse, M. and Niamien, P.M. (2022) Experimental Aspect and Theoretical Modelling of Aluminium Inhibition Corrosion by Vitamins B1, B3 and B6 in Chloric Acid Solution. *American Journal of Applied Chemistry*, **10**, 120-128. https://doi.org/10.11648/j.ajac.20221005.12

[43] Langmuir, I. (1938) Surface Motion of Water Induced by Wind. *Science*, **87**, 119-123. https://doi.org/10.1126/science.87.2250.119

[44] Temkin, M.I. (1941) Adsorption Equilibrium and Process Kinetics on Inhomogeneous Surfaces with Interaction between Adsorbed Molecules. *Zhurnal Fizicheskoi Khimii*, **15**, 296-332.

[45] Frumkin, A. (1925) Die Kapillarkurve der höheren Fettsäuren und die Zustandsglei-

chung der Oberflächenschicht. *Zeitschrift für Physikalische Chemie*, **116**, 466-484. https://doi.org/10.1515/zpch-1925-11629

[46] Elawady, Y.A. and Ahmed, A.I. (1985) Cheminform Abstract: Effect of Temperature and Inhibitors on the Corrosion of Aluminum in 2N Hydrochloric Acid Solution: A Kinetic Study. *Indian Journal of Chemistry-Section A*, **24**, 601-602.

[47] Adejo, S.O., Ekwenchi, M.M. and Iosr (2014) Resolution of Adsorption Characterisation Ambiguity through the Adejo-Ekwenchi Adsorption Isotherm: A Case Study of Leaf Extract of *Hyptis suaveolen* Poit as Green Corrosion Inhibitor of Corrosion of Mild Steel in 2 M HCl. *Journal of Emerging Trends in Engineering and Applied Sciences*, **5**, 201-205.

[48] Eddy, N.O., Momoh-Yahaya, H. and Oguzie, E.E. (2015) Theoretical and Experimental Studies on the Corrosion Inhibition Potentials of Some Purines for Aluminum in 0.1 M HCl. *Journal of Advanced Research*, **6**, 203-217. https://doi.org/10.1016/j.jare.2014.01.004

[49] Kedimar, N., Rao, P. and Rao, S.A. (2023) Ionic Liquid as an Effective Green Inhibitor for Acid Corrosion of Aluminum Composite: Experimental and Theoretical Considerations. *Journal of Applied Electrochemistry*, **53**, 1473-1489. https://doi.org/10.1007/s10800-023-01854-7

[50] Qiang, Y., Zhang, S., Xu, S. and Li, W. (2016) Experimental and Theoretical Studies on the Corrosion Inhibition of Copper by Two Indazole Derivatives in 3.0% NaCl Solution. *Journal of Colloid and Interface Science*, **472**, 52-59. https://doi.org/10.1016/j.jcis.2016.03.023

[51] Prajapati, K., Desai, P.S., Vashi, R.T. and Parmar, B.B. (2024) Investigating the Corrosion Inhibition of Aluminium by Diamine Derivatives in Hydrochloric Acid: A Multi-Technique Approach. *Chemical Papers*, **78**, 7999-8018. https://doi.org/10.1007/s11696-024-03651-8

[52] Zhou, Y., Zhang, S., Guo, L., Xu, S., Lu, H. and Gao, F. (2015) Studies on the Effect of a Newly Synthesized Schiff Base Compound on the Corrosion of Copper in 3% NaCl Solution. *International Journal of Electrochemical Science*, **10**, 2072-2087. https://doi.org/10.1016/s1452-3981(23)04830-7

[53] Tao, Z., Zhang, S., Li, W. and Hou, B. (2009) Corrosion Inhibition of Mild Steel in Acidic Solution by Some Oxo-Triazole Derivatives. *Corrosion Science*, **51**, 2588-2595. https://doi.org/10.1016/j.corsci.2009.06.042

[54] Hirozawa, S.T. (1995) Use of Electrochemical Noise in the Study of Corrosion Inhibition of Aluminum by Gem Diphosphonates. *Proceedings of 8th European Symposium on Corrosion Inhibitors*, University of Ferrara, 18-22 September 1995, 1366 p.

[55] Frisch, M.J., Trucks, G.W., Schlegel, H.B., Scuseria, G.E., Robb, M.A., Cheeseman, J.R., *et al.* (2009). 09, Revision D. 01, Gaussian. Inc., Wallingford, CT.

[56] Tigori, M.A., Koné, A., Allou, N.B., Gaston, K.A., Jean-Jaurès, Z.D., Sissouma, D., *et al.* (2024) 2-(4-fluorobenzyl)chromeno[2,3-c]pyrozol-3(2h)-One as Copper Corrosion Inhibitor in HNO3: Gravimetric and Quantum Chemical Investigation Methods. *Asian Journal of Chemical Sciences*, **14**, 100-113. https://doi.org/10.9734/ajocs/2024/v14i5327

[57] Tigori, M.A., Adingra, K.F., Koné, A., M'Bouillé, C., Sissouma, D. and Niamien, P.M. (2024) Comparative Study of Two Nitroimidazopyridinehydrazone Derivatives Inhibition Action for Aluminum Corrosion in 2M HCl: Experimental and Theoretical Insights. *Chemical Science Review and Letters*, **13**, 7-20.

[58] Bine, F.K., Tasheh, S.N. and Nkungli, N.K. (2021) Corrosion Inhibition of Aluminium

in Gas and Acid Media by Some Chalcone-Based N-(3-Aminopropyl)imidazoles: TD-DFT-Based FMO, Conceptual DFT, QTAIM and EDA Studies. *Computational Chemistry*, **9**, 37-63. https://doi.org/10.4236/cc.2021.91003

[59] Martínez-Araya, J.I. (2014) Why Is the Dual Descriptor a More Accurate Local Reactivity Descriptor than Fukui Functions? *Journal of Mathematical Chemistry*, **53**, 451-465. https://doi.org/10.1007/s10910-014-0437-7

[60] Oyeneyin, O.E., Ojo, N.D., Ipinloju, N., Agbaffa, E.B. and Emmanuel, A.V. (2022) Investigation of the Corrosion Inhibition Potentials of Some 2-(4-(substituted)arylidene)-1h-Indene-1,3-Dione Derivatives: Density Functional Theory and Molecular Dynamics Simulation. *Beni-Suef University Journal of Basic and Applied Sciences*, **11**, Article No. 132. https://doi.org/10.1186/s43088-022-00313-0